

Brewing of Filter Coffee, with Philips Research

Technical Report from MACSI's 2012 Problem-Solving Workshop
with Industry

Report MACSI/ESGI/0033



Mathematics Applications
Consortium for Science
& Industry



www.macsi.ul.ie
00353 (0)61 213013

Brewing of Filter Coffee

Academic Contributors: Cian Booth¹, Cathal Cummins², Mohit Dalwadi³, Paul Dellar³, Michael Devereux², Jeff Dewynne³, John Donohue⁶, Andrew Duncan⁷, Fionn Fitzmaurice¹, Andrew Gordon², Matt Hennessy⁴, John Hinch⁸, Ciaran Hickey⁹, Poul Hjorth¹¹, Teresa Kyrke-Smith⁵, Deborah Leahy¹, William Lee^{2,†}, Eoin Lynch¹, Olivier Mercier¹⁰, Stan Miklavcic¹², Stephen Russell⁶, Len Schwartz¹³, Benjamin Franklin Shoji¹⁴, Piotr Swierczynski¹⁵, Catherine Timoney², Jakub Tomczyk¹⁶, Emma Warneford³.

1 School of Mathematics, Trinity College Dublin. 2 MACSI, University of Limerick. 3 OCIAM, University of Oxford. 4 OCCAM, University of Oxford. 5 Department of Earth Sciences, University of Oxford. 6 National University of Ireland Galway. 7 Mathematics Institute, University of Warwick. 8 DAMTP, University of Cambridge. 9 School of Physics, University College Dublin. 10 McGill University. 11 Department of Mathematics, TU Denmark. 12 Phenomics and Bioinformatics Research Centre, University of South Australia. 13 Department of Mechanical Engineering, University of Delaware. 14 Mangosuthu University of Technology, South Africa. 15 University of Warsaw. 16 University of Wrocław.
† <http://www.ul.ie/wlee>, william.lee@ul.ie.

Industrial Representative: Freek Suijver.
Philips Research, Eindhoven, The Netherlands.
(Dated: March 11, 2013)

Executive Summary. We report progress on mathematical modelling of coffee grounds in a drip filter coffee machine. The report focuses on the evolution of the shape of the bed of coffee grounds during extraction with some work also carried out on the chemistry of extraction. This work was sponsored by Philips who are interested in understanding an observed correlation between the final shape of the coffee grounds and the quality of the coffee. We used experimental data gathered by Philips and ourselves to identify regimes in the coffee brewing process and relevant regions of parameter space. Our work makes it clear that a number of separate processes define the shape of the coffee bed depending on the values of the parameters involved e.g. the size of the grains and the speed of fluid flow during extraction. We began work on constructing mathematical models of the redistribution of the coffee grounds specialised to each region and on a model of extraction. A variety of analytic and numerical tools were used. Furthermore our research has progressed far enough to allow us to begin to exploit connections between this problem and other areas of science, in particular the areas of sedimentology and geomorphology, where the processes we have observed in coffee brewing have been studied.

I. INTRODUCTION

Coffee is a popular beverage made from the roasted seeds (beans) of the coffee plant. The beans are ground and part of their soluble content is extracted by hot water. The resulting solution is called coffee. One way of making coffee is to use a drip filter coffee machine. In this arrangement ground coffee is placed within a filter which is in turn within a conical funnel as seen in Fig. 1. Hot water is poured on the coffee either from a single point or from multiple points.

Philips manufacture coffee machines and are interested in understanding the science of the brewing process with a view to ensuring their products reproducibly create good coffee. As with wines, the chemicals responsible for the smell and taste of coffee are too complex for any scientific instrument to directly measure the quality of coffee. Therefore coffee quality is measured by professional tasters. While carrying out tasting experiments Philips researchers noted a correlation between the final shape of the bed of coffee and the quality of the coffee. The final results of one set of experiments involving a range of grain sizes and brewing conditions are shown in Fig. 2. As can be seen the final shape of the bed depends on whether coarse or fine grains are used, and the way the wa-

ter is added to the coffee, as a single jet or multiple jets from a shower head. The grain size distributions corresponding to fine and coarse ground coffee are illustrated in Fig. 3.

Fig. 4 shows a preliminary attempt to understand these results in the context of a coffee control chart [1]. The control chart classifies coffees by the percentage of coffee solids extracted and the concentration of those solids in the final brew. The line on the figure corresponds to the ratio of liquid to coffee grounds used by Philips in experiments shown in Fig. 2. (Note that the concentrations shown by the line have been corrected for the remaining water left in the filter.) It is interesting to note that the ratio of coffee grounds to liquid used makes it very hard to achieve good coffee, by European standards. Since Philips' tasters said that cases 'b' and 'c' from Fig. 2 were good quality we suggest they lie in the ideal region. Presumably coffee from case 'd' was overextracted placing it in the bitter region. We will discuss case 'a' in more detail below, see section III A.

Fig. 5 shows the (cumulative) volumes of water entering the filter, leaving the filter and held within the filter. As can be seen from the figure there are three separate regimes:

1. Filling. Water fills the filter but does not leave.
2. Steady State. Water enters the filter and leaves at the

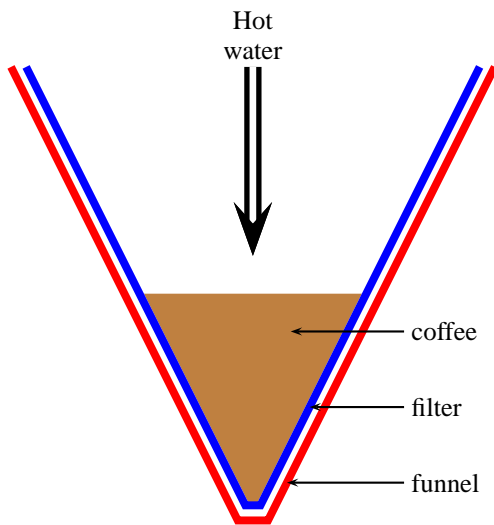


FIG. 1. Arrangement in drip filter coffee. Coffee grounds are placed in filter paper which is in turn placed within a funnel.

same rate.

3. Draining. No more water is added to the filter, but water already held within it drains out.

The report is organised as follows. In Section II we focus on the filling stage, asking the question, “what happens when the water jet or jets hit the grounds?” Here there are two interesting limiting cases, either the jet can punch through the grounds or the water from the jet pools on the surface of the coffee grounds. In Section III we consider how the coffee grounds will distribute themselves in the steady state regime. We identify three cases of interest: (1) the grains are fluidised by the jet which drives a localised circulatory motion, (2) the grains are undisturbed by fluid flow and float on the surface or settle depending on their buoyancy, (3) the grains follow the streamlines of the flow out through the filter which forces them onto the filter. The implications for each of these cases for the final distribution of grains is also discussed. Section IV describes how a model of coffee extraction could be formulated and show a simplified implementation in one dimension. The correct flow equation needed for a range of grain sizes is discussed in Appendix A.

II. INITIAL TRANSIENT

In the very first stages of extraction one or more jets of water strike a dry bed of coffee grains. In our experimental work we observed two different responses to this impact. The first, shown in Fig. 6, is that the jet punches through the fluid. The second is illustrated in Fig. 7 where the water from the jet forms a pool on top of the coffee grounds.

A computational model of the grains using particle dynamics was developed which shows punch through behaviour, this is described in section II A. A model of the deformation of



(a) Coarse grind, single jet.



(b) Coarse grind, shower head.



(c) Fine grind, single jet.



(d) Fine grind, shower head.

FIG. 2. Final shapes of the coffee beds. Strategies (b) and (c) resulted in good coffee, while strategies (a) and (d) resulted in poor tasting coffee.

the coffee bed using thin film flow appropriate for the initial stages of pooling is discussed in section II B.

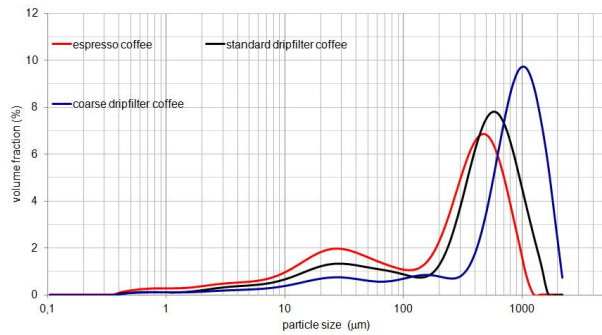


FIG. 3. Grain size distribution in fine (black line) and coarse coffee (blue line). Also shown is the grain size distribution of espresso coffee (red). The smaller peak at $\approx 30 \mu\text{m}$ corresponds to single coffee cells.

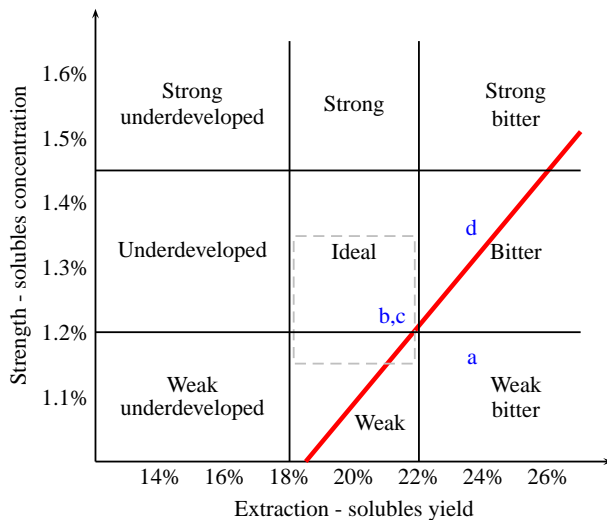


FIG. 4. European coffee control chart [1]. The x -axis shows the percentage of the mass of the coffee grounds extracted. The y -axis shows the (mass) concentration of coffee solids in the resulting solution. The grey dashed line shows the ideal region for American coffee drinkers. The red solid line corresponds to the Philips data. Letters ‘a’ to ‘d’ are our guesses of the locations on the diagram corresponding to the experiments shown in Fig 2.

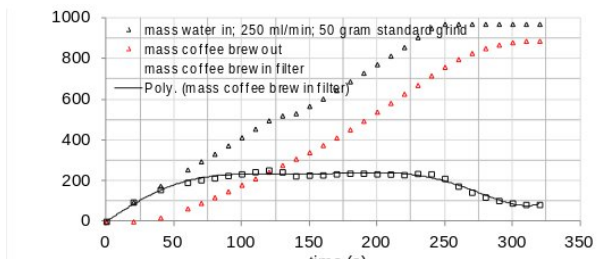


FIG. 5. Cumulative distributions of water entering (black triangles) leaving (red triangles) the filter. Black squares and line show the difference between the two: the amount of water held in the filter.



FIG. 6. If the coffee grounds are weakly held together then a jet of water can punch through the grains as shown here using a half funnel constructed for this purpose.

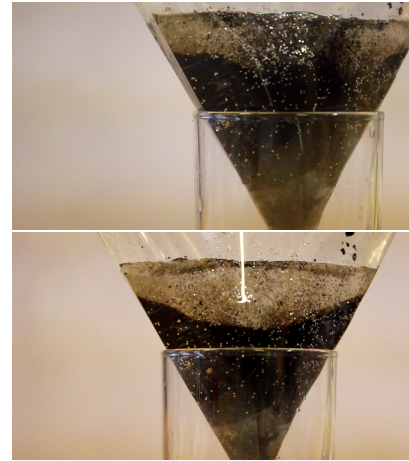


FIG. 7. If jet does not punch through the coffee grounds it instead forms a pool above them.

A. Particle dynamics

A model of the motion of the grains for a strong jet was developed using computational particle dynamics. The simulation, carried out in two dimensions here, proceeds as follows. 1000 grains are placed in a grid pattern over the filter, with their radii distributed around 1 mm. From this initial position the grains are allowed to fall under gravity while interacting with each other to obtain a starting position. Once the grains have reached a stationary position, the effect of turning on the water jet is simulated. To implement the jet a certain region where the water jet hits the grains is identified, and the grains that are at the highest position in this region, i.e. the grains which get a direct impact from the water jet get an additional downwards force applied on them.

During the simulations the state of each particle, dry or wetted, is tracked. Particles are initially dry, and become wetted by either coming into direct contact with the water jet or by prolonged contact with a wetted particle. The motions of the grains are calculated by integrating Newton’s equations $F = ma$ for each grain. The forces included within the simulation include: gravity, a repelling force (damped spring) that is activated if two grains overlap, an attracting force between the wet grains of coffee, water impact. Frames from two sep-

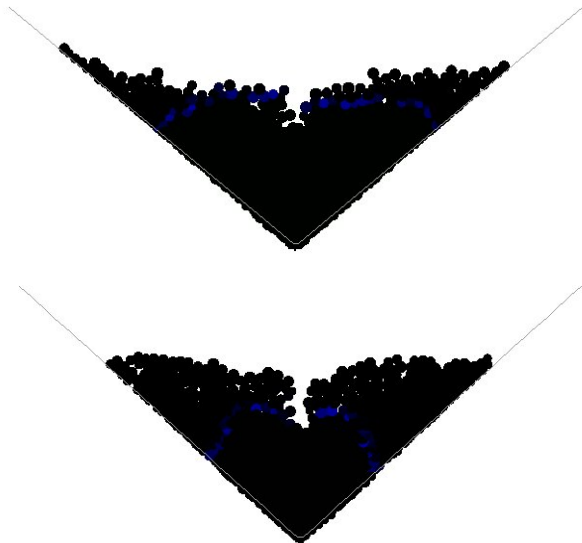


FIG. 8. Frames from two particle dynamics simulations. The interface between wetted and dry particles is shown in blue.

arate simulations are shown in Fig. 8

B. Thin Film model

Here we consider what happens when a droplet of water hits a layer of coffee. In order to model this situation we initially performed some experiments. We filled a filter funnel with coffee, levelled off the coffee surface so that it was roughly flat, and used a pipette to slowly add one drop of water at a time onto the coffee surface. As the droplet hit the coffee, we saw the droplet pick up coffee particles from the coffee bed; the coffee particles then floated to the surface of the droplet; the droplet spread; and finally the droplet was absorbed into the coffee bed, which resulted in the surface of the coffee bed being altered to a “crater-like” shape, the result of one such experiment is shown in Fig. 9. We believe this crater shape is due to the spreading of the droplet before it is absorbed into the coffee bed. This spreading leads to more coffee being taken up by the droplet than deposited at the centre of the drop, whereas more coffee is deposited than taken up at the edge of the spread droplet (as no coffee was initially taken up from that part of the coffee bed surface). We repeated the process of adding one droplet of water at a time onto the coffee, which led to the crater getting deeper and more pronounced.

From the experiments it appears that the droplet spreads on a much faster timescale than the timescale for absorption into the coffee bed. Thus in our model we treat these two processes as completely separate. Our mathematical model is divided into several sections (as depicted in figure 10). Initially we model the droplet hitting the surface of the coffee and taking up coffee particles from the coffee bed, then we model the spreading of the droplet, finally, we model the deposition of the coffee particles onto the surface of the coffee bed, as the



FIG. 9. End result of droplets of water landing on a bed of dried coffee.

droplet is absorbed into the coffee. We present the results obtained from solving our model numerically for repeated drops on to the coffee bed.

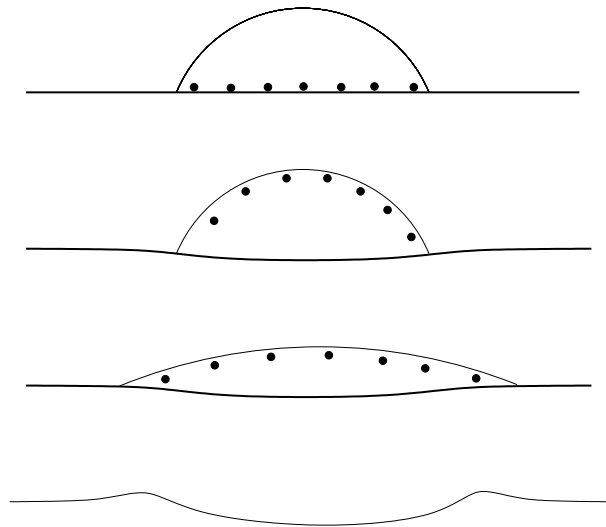


FIG. 10. The distinct stages of our model: initially the droplet of water hits the coffee bed and picks up coffee particles; these particles move to the surface of the droplet; the droplet spreads; finally the droplet is absorbed into the coffee, depositing the coffee that was in the droplet back onto the surface of the coffee bed, and so altering the surface of the coffee bed.

1. Mathematical Model

We consider how a two-dimensional bed of coffee with a surface given by $z = \eta(x)$ evolves when a sequence of water droplets impact the surface, spread out to their equilibrium profile $z = h(x)$, and then sink into the underlying bed, depositing coffee grains as they do so. The contact point, which denotes the point where the surface of the water droplet comes into contact with the coffee, is given by $x = s$. The equilibrium contact angle is denoted by θ . We further suppose that the droplet surface and the coffee surface are symmetric about the z -axis. A schematic diagram with these details is shown in Figure 11.

We decompose the evolution of the surface into two discrete stages. If $\eta_i(x)$ denotes the surface of the coffee bed after the

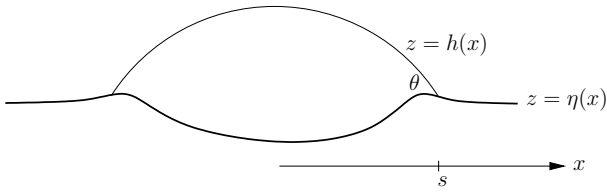


FIG. 11. A droplet of water with equilibrium shape $z = h(x)$ resting on a bed of coffee with a surface $z = \eta(x)$. The contact point and the contact angle are denoted by s and θ , respectively.

i -th droplet has sunk into it, then we first consider the stage where a drop of water impacts this surface and ejects coffee from it, thus creating a new surface $\eta_{i+1/2}(x)$. The droplet spreads over this surface and then sinks into it, depositing coffee grains and creating a new coffee profile given by $\eta_{i+1}(x)$. This simple process can be repeated to determine the overall shape of the coffee bed after multiple drops of hot water have been deposited onto it.

a. Droplet impact and coffee uptake The mathematical details of a droplet impacting a porous substrate are quite complicated and therefore, the first phase that we consider in our model is actually a post-impact stage, where we suppose that the drop of water has already hit the surface and formed a parabolic droplet. This initial droplet will then spread to its equilibrium profile under the action of surface tension and gravity; a process that will be explained below. We work in non-dimensional variables and assume that each initial droplet has a radius of unity and an area of A . If the initial droplet profile is given by $h_{\text{initial}}(x)$, then the first assumption implies $h_{\text{initial}}(1) = \eta_i(1)$, whereas the second assumption implies

$$\int_0^1 [h_{\text{initial}}(x) - \eta_i(x)] dx = A/2. \quad (1)$$

We then take the initial profile to be parabolic and of the form

$$h_{\text{initial}} = B(1 - x^2) + \eta_i(1), \quad (2)$$

where the constant B is given by

$$B = \frac{3}{2} \left[\frac{A}{2} - \eta_i(1) + \int_0^1 \eta_i(x) dx \right], \quad (3)$$

which is a consequence of imposing the condition in (1).

Experiments have shown that when the water drop impacts the surface, coffee grains are ejected from the bed and sent to the surface of the drop. We assume that the amount of coffee that is removed from the bed at a point x is proportional to the height of the initial droplet at that point. This implies the first stage in the coffee bed evolution can be written as

$$\eta_{i+1/2}(x) = \eta_i(x) - \psi[h_{\text{initial}}(x) - \eta_i(x)], \quad (4)$$

where ψ is a constant of proportionality. The total mass that

is removed from the bed is given by

$$m_i = 2\psi \int_0^1 [h_{\text{initial}}(x) - \eta_i(x)] (1 + \eta_{i,x}^2)^{1/2} dx \quad (5)$$

and we assume that this mass is uniformly distributed over the surface of the droplet.

b. Drop spreading After the uptake of coffee from the bed, the drop spreads out. We calculate the final shape the fixed volume droplet makes on our curved substrate. We will take the drop to have a small height to length ratio and hence use lubrication theory with the Navier-Stokes equations. We use Tanner's Law as a boundary condition.

We model the droplet to be two dimensional in the (x, z) -plane and to be a homogeneous, incompressible, Newtonian fluid of density ρ and viscosity μ . The unit vectors in the x and z -directions are e_x and e_z respectively. The droplet lies on the substrate, experiencing a gravitational force g in the negative z -direction. The droplet will spread from its initial shape to a steady state with experimentally determined contact angle θ at the contact point $x = s$, which we will determine in our calculations. The substrate is given by the equation $z = \eta(x)$, and the free surface of the droplet is given by the equation $z = h(x, t)$ (as shown in figure 11.)

The fluid within the droplet is governed by the Navier-Stokes equations with incompressibility equation

$$\rho \left(\frac{\partial \mathbf{u}}{\partial t} + (\mathbf{u} \cdot \nabla) \mathbf{u} \right) = -\nabla p + \mu \nabla^2 \mathbf{u} - \rho g e_z, \quad (6)$$

$$\nabla \cdot \mathbf{u} = 0, \quad (7)$$

where $\mathbf{u} = (u, v)$ is the fluid velocity, p is the fluid pressure, t denotes time and subscripts represent differentiation with respect to that parameter. In 2D and in component form, these equations become

$$\rho(u_t + uu_x + wu_z) = -p_x + \mu(u_{xx} + u_{zz}), \quad (8)$$

$$\rho(w_t + uw_x + ww_z) = -p_z + \mu(w_{xx} + w_{zz}) - \rho g, \quad (9)$$

$$u_x + w_z = 0. \quad (10)$$

On the substrate $z = \eta(x)$ we impose zero slip and flux, on the free boundary $z = h(x, t)$ we impose the kinematic boundary condition, normal stress balancing with surface tension and tangential stress being zero. Hence, on $z = \eta(x)$, we have

$$(u, w) = (0, 0), \quad (11)$$

and on $z = h(x, t)$ we have

$$-uh_x + w - h_t = 0, \quad (12)$$

$$\mathbf{n} \cdot \mathbf{T} \cdot \mathbf{n} = \sigma \kappa, \quad (13)$$

$$\mathbf{n} \cdot \mathbf{T} \cdot \mathbf{t} = 0, \quad (14)$$

where \mathbf{T} is the stress tensor, \mathbf{n} is the outward pointing unit normal to the surface, \mathbf{t} is the positive orientated unit tangent of the surface, σ is the surface tension acting on the fluid surface and $\kappa = -\nabla \cdot \mathbf{n}$ is the curvature of the surface. $\mathbf{T} = (T)_{ij}$

is given by

$$\mathbf{T} = -\mathbf{I}p + \mu(\nabla\mathbf{u} + (\nabla\mathbf{u})^T), \quad (15)$$

where \mathbf{I} is the identity matrix.

We will also have boundary conditions due to symmetry. These are

$$h_x(0, t) = 0, \quad (16)$$

$$h_{xxx}(0, t) = 0. \quad (17)$$

The point at which the drop leaves the substrate is denoted by $x = s(t)$. The boundary conditions that relate to this are the contact boundary condition and Tanner's Law

$$h(s, t) = \eta(s), \quad (18)$$

$$s_t = -(h_x(s, t) - \eta_x(s))^3 - \theta^3. \quad (19)$$

In the steady state, the last boundary condition becomes

$$h_x(s^*) = \eta_x(s^*) - \theta, \quad (20)$$

where s^* is the steady position of s .

Our final boundary condition is a constant volume boundary condition. Since we are working in two dimensions we take the volume of the initial drop to be denoted by A . Therefore we have

$$\int_0^{s(t)} [h(x, t) - \eta(x)] dx = A/2. \quad (21)$$

In the steady state, this becomes

$$\int_0^{s^*} [h(x) - \eta(x)] dx = A/2, \quad (22)$$

We non-dimensionalise as follows

$$\left. \begin{aligned} x &= Lx', \\ z &= Hz', \\ (u, w) &= U(u', \epsilon w'), \\ t &= \frac{L}{U}t', \\ (p, \mathbf{T}) &= \frac{\mu U}{\epsilon H}(p', \mathbf{T}'), \end{aligned} \right\} \quad (23)$$

where L is the typical length of the drop, H is the typical height of the drop, U is the typical velocity scale of the drop (and $U = (\epsilon^3\sigma)/\mu$ but this will be determined later) and $\epsilon = H/L \ll 1$ is the small ratio between typical height and length. Substituting into our governing equations (8) - (10), we find (dropping the ')

$$\epsilon^2 Re(u_t + uu_x + wu_z) = -p_x + \epsilon^2 u_{xx} + u_{zz}, \quad (24)$$

$$\epsilon^4 Re(w_t + ww_x + ww_z) = -p_z + \epsilon^4 w_{xx} + \epsilon^2 w_{zz} - B, \quad (25)$$

$$u_x + w_z = 0, \quad (26)$$

where $Re = (\rho UL)/\mu$ is the Reynolds number, a ratio of inertial to viscous forces, and $B = (\epsilon^3 L^2 \rho g)/(\mu U) = (L^2 \rho g)/\sigma$ is the Bond number, a ratio of gravitational to surface tension forces. Physically, we have $B = O(1)$. We will also assume that the reduced Reynolds number, $\epsilon^2 Re \ll 1$. At leading order in ϵ^2 and $\epsilon^2 Re$, this becomes

$$0 = -p_x + u_{zz}, \quad (27)$$

$$0 = -p_z - B, \quad (28)$$

$$u_x + w_z = 0, \quad (29)$$

At leading order, the boundary conditions on the free surface $z = h(x, t)$ become

$$-uh_x + w - h_t = 0, \quad (30)$$

$$-p = h_{xx}, \quad (31)$$

$$u_z = 0, \quad (32)$$

and the other all stay the same.

Our goal is to find a governing equation for the droplet's surface, h . To proceed, we use a standard averaging procedure and integrate with respect to z from η to h , hence equation (29) becomes

$$\frac{\partial}{\partial x} \int_{\eta}^h u dz - h_x u(h, t) + \eta_x u(\eta, t) + w|_{z=\eta}^h = 0. \quad (33)$$

Using boundary conditions (11) and (30), this becomes

$$\frac{\partial h}{\partial t} + \frac{\partial}{\partial x} \int_{\eta}^h u dz = 0. \quad (34)$$

We now need to solve (27) and (28) for u so we can substitute this into equation (34).

We can solve (28) with boundary condition (31) to find

$$p(x, z, t) = B(h - z) - h_{xx}. \quad (35)$$

Substituting this into equation (27), we find

$$Bh_x - h_{xxx} = u_{zz}, \quad (36)$$

which is easily solved for u , using boundary conditions (11) and (32) to find

$$u = \frac{1}{2} (Bh_x - h_{xxx}) (z^2 - 2hz + 2\eta h - \eta^2). \quad (37)$$

We now substitute this into equation (34) to find our governing equation for the surface

$$\frac{\partial h}{\partial t} - \frac{1}{3} \frac{\partial}{\partial x} ((h - \eta)^3 (Bh_x - h_{xxx})) = 0. \quad (38)$$

We now assume that the drop has a steady state solution governed by the steady form of equation (38), and the boundary conditions (16) - (18), (20) and (22).

The steady state form of (38) and symmetry boundary con-

ditions (16) and (17) yield

$$Bh_x - h_{xxx} = 0, \quad (39)$$

which can be solved using the symmetry boundary conditions again to give

$$h = A + \frac{C}{\sqrt{B}} \cosh(\sqrt{B}x), \quad (40)$$

where A and C are constants of integration. We will drop the asterisks from s^* for convenience as we are working in the steady state. The boundary condition (18) gives

$$A = \eta(s) - \frac{C}{\sqrt{B}} \cosh(\sqrt{B}s), \quad (41)$$

and using this in boundary condition (20) gives

$$C = \frac{\eta_x(s) - \theta}{\sinh(\sqrt{B}s)}. \quad (42)$$

We have a final boundary condition to use so we can find s , the x -value at which the steady state drop first comes off the substrate η . We use boundary condition (22) to deduce that s satisfies the implicit equation

$$\begin{aligned} A/2 - s\eta(s) + \int_0^s \eta(x) dx \\ = \frac{\eta_x(s) - \theta}{B} \times [1 - s\sqrt{B} \coth(\sqrt{B}s)] \end{aligned} \quad (43)$$

Hence, our final drop shape is given by

$$\begin{aligned} h(x) = \eta(s) + \frac{\eta_x(s) - \theta}{\sqrt{B} \sinh(\sqrt{B}s)} \times \\ \left[\cosh(\sqrt{B}x) - \cosh(\sqrt{B}s) \right], \end{aligned} \quad (44)$$

where s is defined implicitly by equation (43).

c. Coffee deposition After the droplet has spread to its equilibrium profile, it will begin to seep into the porous bed of coffee below. The precise details of the seepage process are beyond the scope of this study and hence they are neglected. Instead, we suppose that the seepage process merely deposits the coffee grains on the surface of droplet directly to the underlying surface of the coffee bed. By maintaining the assumption that the coffee grains are uniformly distributed over the surface of the droplet, the surface density of coffee is given by

$$\lambda_i = \frac{m_i}{2 \int_0^s (1 + h_{i,x}^2)^{1/2} dx}, \quad (45)$$

where m_i is the mass of coffee that is ejected during the impact stage (see (5)). The incremental amount of coffee contained within a droplet surface element ds_d is then $dm = \lambda_i ds_d$. If this mass of coffee is deposited directly onto the

bed surface element below, denoted as ds_b , then the change in bed height, $\Delta\eta$, is given by $\Delta\eta ds_b = dm = \lambda_i ds_d$. It should be noted that if dimensional quantities were used, the left-hand side of this expression would be multiplied by the (area) density of coffee. By rewriting the surface elements of the bed and the droplet in terms of the element dx , the final shape of the coffee bed can be written as

$$\eta_{i+1}(x) = \eta_{i+1/2}(x) + \lambda_i \frac{(1 + h_{i,x}^2)^{1/2}}{(1 + \eta_{i+1/2,x}^2)^{1/2}}. \quad (46)$$

2. Results

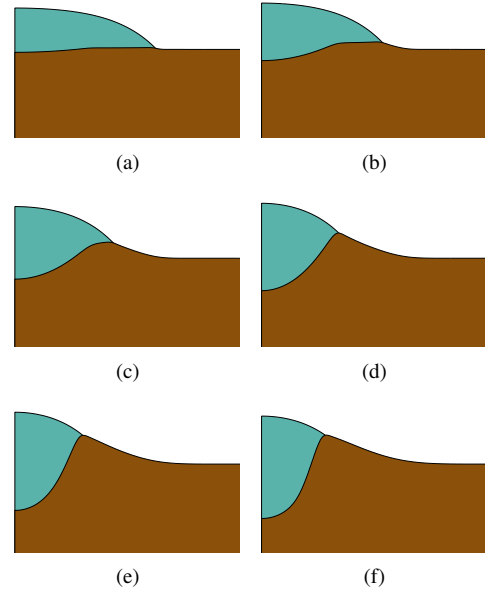


FIG. 12. Results are shown for the droplets 1, 4, 8, 15, 30 and 50. The shape of the droplet before it sinks into the coffee bed is shown in blue, and the final shape of the coffee bed after that droplet has taken up coffee, spread out, and redeposited the coffee is in brown. Note that results are shown on just one side of the axis of symmetry.

We developed a simple Matlab script to solve (43) for s and (44) for the final drop shape $h(x)$. The coffee uptake is governed by (4) and the deposition by (46). The contact angle θ is taken to be 50° .

Figure 12 illustrates the solutions after various number of droplets have fallen. The final shape, $h(x)$, of the droplet pre-absorption is shown in blue and the resulting shape of the coffee bed due to the coffee being redeposited in brown. The coffee bed is initially flat. Figure 12(a) shows that after the first drop lands, spreads, and deposits the coffee it had taken up as it landed, a slight crater immediately forms. This is due to the fact that more coffee was taken up from part of the bed where the drop landed than was re-deposited there. As more drops then land the crater-like structure with a raised rim becomes more emphasised due to the cumulative effect of all of

the droplets spreading and redepositing the coffee. Eventually a steady state is reached. Droplets land in the crater that has formed, and cannot spread out due to the bed shape. This results in deposition of the coffee entrained as the droplet lands in the same place, and so no change of shape of the coffee bed.

We use a very simplified model for this work. We chose to work with a series of distinct droplets which spread due to gravity and capillary effects. This still tells us useful information about how the coffee bed might deform, as seen above. Some things to think about for future work, however, include

- The contact angle of 50° is somewhat arbitrary. It would therefore be useful to carry out a set of experiments to determine what the contact angle for hot water on coffee is.
- Can we compute the steady state crater shape more explicitly? In our simulations we tend towards a steady state but it would be useful to find an explicit equation to solve for the steady state.

III. STEADY STATE

According to Fig. 5 the majority time the coffee is brewing occurs in a steady state regime. It seems likely that the behaviour of the coffee grounds and water during this period has the largest effect on the quality of the coffee produced.

In our experiments we identified three types of behaviour which could occur in the steady state regime, depending on the dominant velocity scale of the system. These velocity scales are:

1. Jet velocity $\approx 1 \text{ m s}^{-1}$ for a single jet.
2. Stokes velocity, mm s^{-1} to cm s^{-1} , the velocity with which a particle moves relative to the fluid because of its weight or buoyancy.
3. Filtration velocity, mm s^{-1}

A. Jet dominated flow

If the most important velocity scale in the system is the velocity of the jet then the grains will follow the flow pattern set up by the jet. Fig. 13 shows an experimental realisation of this case. The system initially consisted of layers of couscous and coffee, to which a jet of cold water was applied. As the figure shows there is a localised region of circulation (which can be seen by coffee grounds brought to the surface) surrounded by a quiescent region. We suggest that overextraction occurs within the region of circulation while underextraction occurs within the quiescent region, the upper parts of which may not even be wetted in practice. We therefore expect—in the terminology of Fig. 4—a weak, overextracted coffee in the case of jet dominated flow (case ‘a’ in Fig. 2). The final shape adopted by the coffee bed will be determined by the configuration adopted by the grains in the absence of the jet.



FIG. 13. Jet dominated flow. There is a local region of circulation driven by the jet with stagnant edges.



FIG. 14. Coffee grains initially float on water and then sink. The process can be accelerated by using soapy water containing washing up liquid and retarded by using cold water.

B. Stokes velocity dominated flow

Since the coffee grounds do not have the same density as water they will tend to move either upwards or downwards relative to the streamlines. If the velocity associated with this motion is larger than the other velocity scales in the system then this will determine their distribution. This is what is observed for instance in a cafetiere. Our experiments suggest that coffee grains can be both less dense and denser than water, see Fig. 14.

While it is obvious that part of the buoyancy of coffee grains comes from the release of CO_2 which occurs when they are wetted it is not obvious whether this is the only factor responsible for their change in buoyancy. The transfer of soluble compounds from the grains to the liquid may also result in a change in buoyancy. The role the washing up liquid plays in accelerating the decrease in the buoyancy of the grains is also unclear. It may increase the solubility of the water to hy-



FIG. 15. If the dominant velocity scale of the system is the filtration velocity then coffee grains will follow streamlines until they intersect the filter.

drophobic coffee compounds or it may allow escaping gas to form smaller bubbles which more easily detach from grains.

If grains float on the surface during the steady state regime then their final distribution will be determined by slumping as the layer of water supporting them drains away.

C. Filtration velocity

A final possibility is that the largest velocity scale in the steady state regime is the filtration velocity. In this case coffee grains follow streamlines until they intersect with either the filter paper or coffee grounds overlaying the paper. Fig. 15 illustrates this case.

We developed an analytic model and a numerical procedure for modelling this case.

1. Analytic Model

We seek to predict the shape of the coffee ground wall distribution in a conical paper filter after a measured quantity of hot water is poured into the filter and allowed to drain through the grounds and the filter into a carafe. Graphs, parameter values, and movies were provided. A particular set of graphs showed the weight of the cone versus time as a total of one litre of water was poured, at a steady rate, into 50 grams of dry ground coffee. The pour time varied from 4 to 8 minutes. After all the liquid was poured, the weight data was continued until the weight was again equal to about 50 grams, indicating that all the water had been drained. Each curve had three distinct phases: (i) weight increasing monotonically until it reaches a value of about 200 grams, (ii) a steady-state region where the weight stays approximately constant until all the water has been poured. This indicates the rate of outflow through the filter is equal to the inflow rate, and (iii) the final time interval, after pouring has stopped, when the weight falls, asymptotically approaching the original 50 grams.

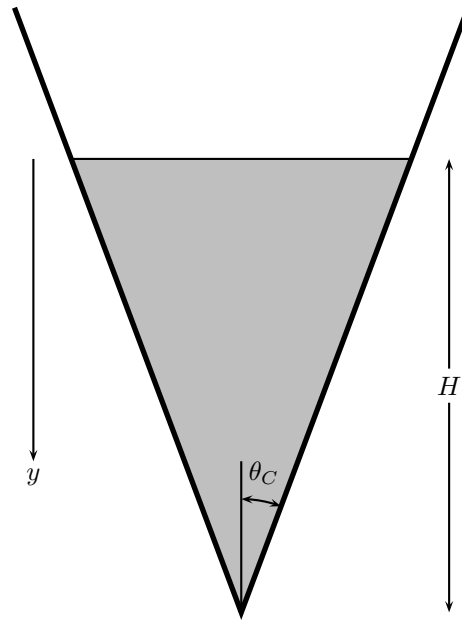


FIG. 16. The filter is a vertical cone of half-angle θ_c .

In order to arrive at a prediction, we need to know the time dependent flow field. This is a difficult problem because we need to consider the rheology of a slurry whose composition varies in space and time as well as the details of the pouring.

It would seem clear however that the flow is driven, at least to some extent, by hydrostatic pressure. This could correspond to a limiting case where the filling flow is uniform over the free liquid surface and the fall height of the inflow is made as small as possible to minimise kinetic energy input. In such a limit the liquid free surface would be horizontal in the cone. (a) Thus we will assume quasi-static flow. This would not seem unreasonable since the order-of-magnitude of the free surface height movement is about 1 cm/minute. This suggests a Reynolds number

$$\text{Re} = \frac{\rho V D}{\mu} \quad (47)$$

between 1 and 10 for a diameter $D = 5$ cm and a viscosity between one and 10 cp. A representative Froude number

$$\text{Fr} = \frac{V^2}{gD} = O(10^{-7}) \quad (48)$$

suggesting that dynamic pressures are very much smaller than hydrostatic for most of the flow.

(b) We will assume that the slurry is uniformly mixed and that the specific gravity of the coffee grains is one. Thus, if small enough, they can be expected to act as passive tracers in the flow. Apparently the grains are buoyant when dry but become heavier as they soak, suggesting that neutral buoyancy is not an unreasonable assumption.

(c) The flow through the filter paper is simply proportional to the pressure difference across the paper which is $\rho g y$, where y is measured downward from the instantaneous liquid free

surface.

(d) particles are trapped and remain attached to the inside of the filter. Successive particles attach to earlier ones, thereby building up the particle “cake” at any given location. While it is likely that the cake buildup reduces the permeability over time, we ignore that effect here.

We will not treat phase (i) above which is the filling phase. Clearly it is the most difficult of the three sub-problems since it involves fluidising the initial dry powder. We do feel that it also can be simplified somewhat in the slow flow limit.

The contribution from steady-state phase (ii) is most easily seen if we were to continue this phase indefinitely until all the particles are deposited and the exiting water runs clear. (This would of course lead to a large quantity of very weak coffee.) The final dry slurry profile would be a simple linear increase from zero thickness at the level of highest rise in the cone, H_0 say, which is perhaps twice the level of the initial dry powder using the numbers given above. The thickness profile is simply

$$\delta(y) = K_1 y \quad (49)$$

where y is measured downward from H_0 . The linear curve needs to be terminated at the cone centre line. The value of K_1 is found by requiring the volume enclosed between the two cones (i.e. the filter cone and the slurry surface) to be equal to the known volume of wet grounds, say 50 cm^3 here.

The draining phase (iii) is a bit more complicated. At a particular time when the liquid level is at $H < H_0$, we balance the rate of volume change in the cup to the volumetric outflow rate, driven hydrostatically, through the filter cone below H . Thus

$$Q = -\pi R^2 \frac{dH}{dt} \quad (50)$$

$$= -\pi \tan^2 \theta_c H^2 \frac{dH}{dt} \quad (51)$$

$$= \int_0^H dQ \quad (52)$$

$$= K_2 \frac{\tan \theta_c}{\cos \theta_c} \int_0^H (H - y) y dy \quad (53)$$

leading to

$$\frac{dH}{dt} = -\frac{K_2 H}{\sin \theta_c}. \quad (54)$$

Since $H(0) = H_0$, the level falls as

$$\frac{H}{H_0} = \exp\left(-\frac{t}{t^*}\right) \quad (55)$$

where t^* is a characteristic time. But $H = H_0 - y$, and using equation 54, we obtain

$$\delta_3(y) \sim \int y dt = -K_3 [\log(1 - z) + z] \quad (56)$$

where $z \equiv y/H_0$. Note that the quantity in brackets behaves like $\frac{1}{2}z^2$ for small z and becomes positive infinite as $z \rightarrow 1$.

Thus finally the predicted profile of dried coating on the filter, due to phases (ii) and (iii), will be

$$\frac{\delta(z)}{H_0} = Az + B [\log(1 - z) + z] \quad (57)$$

where the new constants A and B will be determined by the volume constraint and a measure of the relative time spent in the two phases which probably can be determined most easily from experiment.

A schematic diagram showing the contributions of the two phases is in Fig. 17. A frame from a Philips movie during drainage, in Fig. 2(d), seems to be in qualitative agreement with the hydrostatic theory developed here.

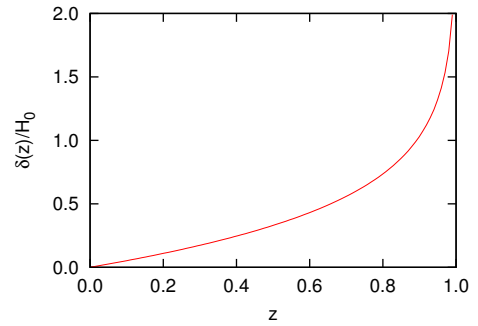


FIG. 17. Diagram showing the final fully-drained shape of the slurry, from equation 57.

2. Numerical Approach

An alternative numerical treatment of the same problem is possible, presented here for a simplified geometry and flow field. The advantages of this approach are: it allows for a more general initial distribution of grain locations; the effects of grain motion relative to the streamlines can be included via the stokes velocity; inclusion of the stokes velocity also allows the effect of a range of grain sizes to be included.

The geometry used in this approach is a two dimensional version of the cone, illustrated in Fig. 18. The velocity field of the water is taken to be: $v_x = ax, v_z = -az$ where: $a = \frac{Q}{dLh}$,

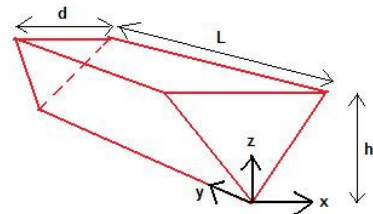


FIG. 18. Geometry.

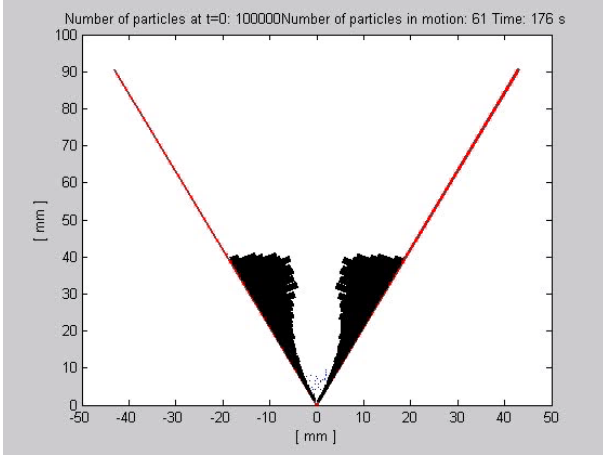


FIG. 19. Numerical calculation of the distribution of the coffee grounds on the surface of the filter.

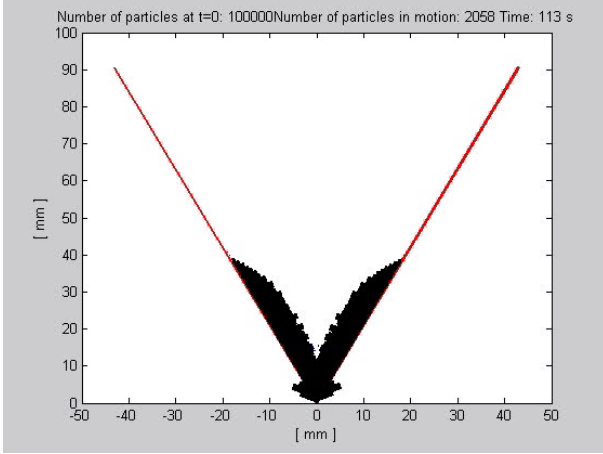


FIG. 20. Numerical calculation of the distribution of coffee grounds using higher Stokes velocities.

and Q is flux of water through the cone. Coffee grounds move relative to the flow field with a velocity given by Stokes Law

$$v_s = \frac{2}{9} \frac{(\rho_p - \rho_f)}{\mu} g r^2$$

where ρ_p is the mass density of the particles, ρ_f is the mass density of the fluid, μ is the dynamic viscosity, r is radius of the particle, and g is acceleration due to gravity.

Simulations are started with 100000 particles with diameters distributed according to particle size distribution of standard coffee. Particle trajectories are calculated until they intersect with the filter paper whereupon they become attached. A histogram of attachment locations is built up over the simulation. Fig. 19 shows the final distribution of particles for a standard simulation. Fig. 20 shows the effect of increasing the stokes velocity by a factor of 4, i.e. simulating the effect of denser particles or a slower filtration velocity.

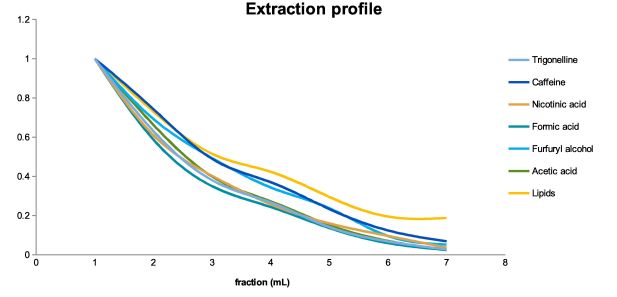


FIG. 21. Philips' own research suggests that a large number of compounds found in coffee are extracted with similar kinetics.

IV. EXTRACTION MODELS

As noted above coffee extraction is a complex and poorly understood process on the chemical level. While Philips' own research suggests that a large number of chemicals are all extracted at approximately the same rate, see Fig. 21, other classifications [2] suggest four groups of chemicals with different extraction kinetics due to their increasing molecular weight. In order of speed of extraction these are

1. Delicate: fruits and floral.
2. Mid times: wood, nuts etc.
3. Sweet: caramel, vanilla etc.
4. Bitter: clove, tobacco etc.

For an ideal cup of coffee only the first three components should be extracted.

Here we report preliminary results towards a model of coffee extraction. We consider only a single component (or multiple components with the same kinetics) and one dimensional flow.

A. One Dimensional Coffee Extraction

To include coffee extraction within the standard equations of porous medium flow we include an equation for transport of coffee.

$$\frac{\partial \rho \omega_C}{\partial t} + \nabla \cdot (\rho v \omega_C) = A_1 (\omega_g - \omega_C) \quad (58)$$

We assume the transport of coffee is advection dominated so we do not include a diffusion term. ρ is the density of the liquid, ω_C is the (mass) concentration of coffee, v is velocity, ω_g is the concentration of coffee in the grains, A_1 is a coefficient which describes the kinetics of transfer of coffee from the grains to the liquid.

We also include an equation to track the decrease in coffee concentration within the grains.

$$\frac{d}{dt} \omega_g = -A_2 (\omega_g - \omega_C) \quad (59)$$

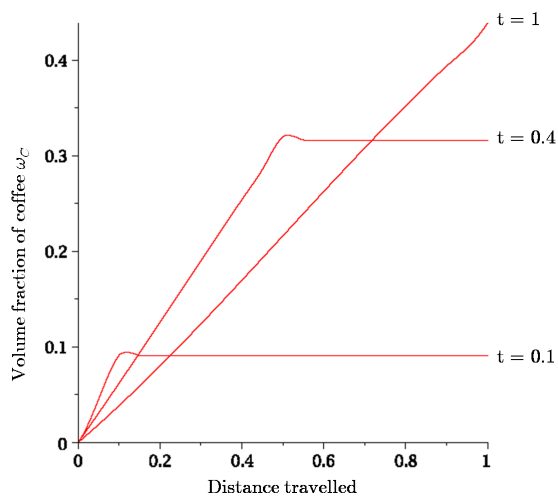


FIG. 22. Numerical solution of coffee extraction equations 58 and 59.

Since the grains are assumed stationary we have a simple, non-convective, time derivative. A_2 describes the kinetics of the transfer.

Numerical solutions of these equations are shown in Fig. 22.

V. CONCLUSIONS

A. Progress

- By using a combination of experimental and theoretical analysis we have identified relevant regimes in the first two stages of the coffee extraction process.
- We have begun work on developing mathematical models appropriate for the various regimes. These models are in varying stages of development.
- We have also started work on a model of coffee extraction.
- Our results suggest that a sophisticated mathematical model of coffee extraction can be constructed.

B. Further Work

a. Initial Transient More work is needed on understanding the rheology of dry and wet beds of coffee grains, and the dependence on rheology on the particle size distribution. This is an area that has been looked at in some detail in the context of geomorphology where the deformation of granular materials by wind, rain, river flow and glaciers has been studied in some detail. For example studies have been carried out on the effect of rainfall on surface [3] and underwater [4] sediments.

b. Steady State Each of the three regimes identified requires further investigation. The flow patterns set up by *jet dominated flow* need to be understood in more detail. One complication absent from our experimental work but clearly present in Philips' experiments (coarse grains, single jet) is the modification of the flow patterns by the release of gasses. An important factor that must be addressed in models of filtration velocity dominated flow is the resistance of layers of coffee grounds to flow. The models used above neglect this effect, appropriate if the resistance of the filter paper to flow is much larger than that of layers of coffee grains. In fact data provided by Philips shows that the reverse is true. Models of *buoyancy dominated flow* require a more detailed understanding of the factors changing the density of grains from less than that of water to above that of water, and how the kinetics of these processes compares with the timescales of coffee extraction.

c. Extraction Models The model of extraction we have created is very simple. To improve it we need more understanding of processes occurring on the scale of a single grain. In particular what limits the kinetics of dissolution of the various components of the coffee? Is it the hydration of the grain or the solubility of those components? Can all components be treated independently or can the presence of one compound limit the solubility of others?

Appendix A: Kozeny-Carman for bimodal size distributions

The particle size distributions, Fig. 3, indicate that the distribution roughly has two modes. Although the coarse grains (approx. 1000 μm) dominate the mixture, it might be possible that the fine grains (approx. 30 μm) cause a non negligible increase in flow resistance. The Kozeny-Carman equation provides a means of estimating the permeability in terms of the average particle diameter $d_{p,av}$ and hydrodynamic porosity ϵ_h of the granules. Various literature on mixtures with bimodal diameter distributions suggest that for high coarse, low fine mixtures the use of the geometric mean (weighted with fraction sizes) is a better choice for the "representative" particle diameter [5, 6].

For a bimodal mixture, we expect the porosity to lie within the upper and lower bounds given by

$$\phi_{ub} = b_{vc}\phi_c + b_{vf}\phi_f, \quad (\text{A1})$$

and

$$\begin{aligned} \phi_{lb} &= \phi_c - b_{vf}(1 - \phi_f) & \text{if } b_{vf} < \phi_c \\ \phi_{lb} &= b_{vf}\phi_f & \text{if } b_{vf} \geq \phi_c, \end{aligned} \quad (\text{A2})$$

where ϕ_c, ϕ_f are the (measured) porosities of the coarse and fine components, b_{vc}, b_{vf} are the fractions of the coarse and fine component respectively (such that $b_{vc} + b_{vf} = 1$).

ϕ_{ub} corresponds to the "zero-mixing" model (particles packed without mixing), whereas ϕ_{lb} corresponds to the "idea mixing model" (all fines are contained within voids of the coarse). The measured porosity would typically lie in between

these bounds depending on the mixing procedure, shape of particles.

for Science and Industry (<http://www.macsi.ul.ie>) funded by the Science Foundation Ireland Mathematics Initiative Grant 06/MI/005.

ACKNOWLEDGMENTS

C. Cummins, A. Gordon, W. Lee and C. Timoney acknowledge support of the Mathematics Applications Consortium

-
- [1] Specialty Coffee Association of Europe. "Coffee brewing control chart." http://scae.com/images/PDF/coffee_brewing_control.pdf.
 - [2] Galla Coffee Blog. "What is overextracted and underextracted coffee." <http://www.gallacoffeeblog.co.uk/overextracted-coffee/>
 - [3] P. I. A. Kinnell. "Raindrop-impact-induced erosion processes and prediction: a review." *Hydrological Processes* **19**:2815–44 2005.
 - [4] T. Green and D. Houk. "The resuspension of underwater sediment by rain." *Sedimentology* **27**:607–610 1980.
 - [5] C. E. Koltermann, S. M. Gorelick. "Fractional packing model for hydraulic conductivity derived from sediment mixtures." *Water Resources Research* **31**:3283–97 1995.
 - [6] Z. F. Zhang, A. L. Ward and J. M. Keller. "Determining the Porosity and Saturated Hydraulic Conductivity of Binary Mixtures." Technical Report PNNL-18801, prepared by Pacific Northwest National Laboratory for the United States Department of Energy.